**METHODS**

# A Method for Evaluating the Impact of Controllers and Wind Turbine Generators on Low-Frequency Oscillation

**QINGBO ZHANG [1], DEQIANG GAN [1], (Senior Member, IEEE), ZHEMING ZHANG[2], JINQIU LI[2], AND YAO LUO[2]**
[1]College of Electrical Engineering, Zhejiang University, Hangzhou 310058, China
[2]Yunnan Power Grid Corporation, Kunming 650011, China

Corresponding author: Qingbo Zhang (zhangqingbo@zju.edu.cn)

**ABSTRACT** Based on the celebrated Generalized Nyquist Criterion, this paper presents a new frequency-domain method to analyze the impact of governor-turbine systems (GTSs), power system stabilizers (PSSs) and wind turbine generators (WTGs) on small disturbance stability in power systems. Compared with other common analysis method, the new method can avoid the calculations of eigenvalues, eigenvectors and residues, and the impact of multiple controllers or WTGs can be obtained using simple matrix operations. In addition, the method is intuitive for users since the stability analysis results can be displayed in the complex plane directly. The new method indicates that the impact of controllers and WTGs on power system is determined by the phase of certain elements in the transfer function matrices of controllers, WTGs and synchronous grid. Based on the information provided by the afore-mentioned transfer function matrices, the parameters of controllers can be optimized properly. The proposed method has been tested using the data of a four-machine two-area system and a regional power grid in China. The results demonstrate that the effect of controllers and WTGs can be conveniently identified, and the effectiveness of parameter tuning for controllers is verified.

**INDEX TERMS** Frequency response, governor-turbine systems (GTS), low-frequency oscillation (LFO), power system stabilizers (PSS), wind turbine generator (WTG).

## I. INTRODUCTION

Low-frequency oscillation (LFO) is one of the most typical small-signal stability problems in modern power systems [1]. The most popular analysis methods for the problem are modal analysis method [2], [3], [4], [5], [6] and damping torque analysis method [7], [8], [9], [10], [11], [12], [13], [14]. The former provides eigenvalues, eigenvectors, by which the information such as frequency, damping ratio, participation level, etc., can be obtained. Furthermore, the eigenvalue sensitivity technique and residues can be employed to analyze the impact of single parameter variation on damping ratio,

The associate editor coordinating the review of this manuscript and approving it for publication was Siqi Bu [ID].

as well as the parameter tuning of power system controllers. The latter is first proposed for the single-machine infinite-bus system, which explains the physical mechanism of LFO well through deriving the relation between damping torque coefficient and damping ratio of oscillation mode. After that, the method of damping torque analysis has been extended to multi-machine power system to perform power system stabilizer design.

Power system stabilizer (PSS) is one of the most effective controllers for suppressing LFO [1]. Identifying the effect of PSSs and optimizing the parameters of PSSs have always been the subjects of major concern in the field. In [15], a modal decomposition method for PSS tuning is proposed, which eliminates the interaction among different modes and

provides sufficient damping for interarea mode of concern. Reference [16] develops a computation time-saving transfer function and eigenfunction analysis method by means of eigenvalue sensitivity concept for coordinated tuning of the PSS of large power systems. The research progress of using PSS to enhance interarea mode damping of longitudinal power system is performed in [17]. A method of coordinated design of multiple PSSs in multi-machine power system which is developed from damping torque method is reported in [18]. Governor is another essential controller which can affect LFO. Reference [19] focuses on the contribution of hydro and steam-turbine governors on oscillation damping, where eigenvalue sensitivities are applied.

In addition to PSSs and governor-turbine systems (GTSs), the impact of the integration of WTGs on small-disturbance stability is another research hotspot in recent years. Due to the high penetration of wind power, the dynamic interaction brought out by WTGs becomes a new affecting factor for LFO. References [20], [21], [22], [23], [24], and [25] compare the electro-mechanic mode before and after the integration of WTGs. Modal analysis method is adopted in [22] and participation factors are computed to acquire the extent to which the WTGs participate in LFO. However, the participation factors can not reflect that whether the impact of integration is positive or negative. Compared with that, [26] develops an approach to convert WTGs into equivalent synchronous machines and evaluates the sensitivity of eigenvalue with respect to inertia. A method based on damping torque analysis is proposed in [27], the impact of two factors including the change of load flow and dynamic interaction introduced by DFIG is examined separately. On the basis of [27] and [28] derives the sensitivity of electromechanical oscillation mode to the dynamic interactions introduced by DFIG.

The main analysis methods for LFO require the calculation of eigenvalues, eigenvectors and residues. Furthermore, it is difficult to distinguish the effect of multiple controllers and multiple WTGs without repeated calculations. A new Nyquist-type method based on frequency response is proposed in this work, it can be utilized to analyze the effect of PSSs, GTSs and WTGs on power system stability. The method can avoid the calculation of eigenvalues, eigenvectors and residues, only frequency response matrices of PSSs, GTSs, WTGs and synchronous grid are required. In addition, the method facilitates the calculation and analysis since the impact of controllers and WTGs can be obtained by simple matrix operations. The parameters of controllers can also be optimized with reference to the analysis results.

The paper is organized as follows. Section II develops the feedback interconnection model of power system with the installation of GTSs and PSSs, and the feedback interconnection model of power system with the integration of WTGs. Based on that, the new method is proposed in Section III, where the rank of loop transfer function matrix of the feedback interconnection model is proved to be approximately equal to 1 at the frequency of low-frequency oscillation.

Then the property is utilized to identify the impact of GTSs, PSSs and WTGs on stability margin. The effectiveness of the proposed method is verified in Section IV, where the effect of GTSs and PSSs in four-machine two-area system, and the effect of WTGs in a regional power grid in China is investigated.

Some preliminary results of this work have been introduced in [29], on the basis of which, the versatility of the proposed method is further developed with abundant analytical findings in this paper.

## II. THE FEEDBACK INTERCONNECTION MODELS

In this section, the feedback interconnection model of power systems with the installation of GTSs and PSSs, and the feedback interconnection model of power systems with the integration of WTGs are introduced.

### A. THE FEEDBACK INTERCONNECTION MODEL OF POWER SYSTEMS WITH GOVERNOR-TURBINES SYSTEMS AND POWER SYSTEM STABILIZERS

Firstly, the linearized state-space model of controllers including GTSs and PSSs in a power system is shown as follows:

$$\begin{bmatrix} s\Delta \boldsymbol{X}_c \\ 0 \end{bmatrix} = \begin{bmatrix} \boldsymbol{J}_{11} & \boldsymbol{J}_{12} \\ \boldsymbol{J}_{21} & \boldsymbol{J}_{22} \end{bmatrix} \begin{bmatrix} \Delta \boldsymbol{X}_c \\ \Delta \boldsymbol{Y}_c \end{bmatrix} + \begin{bmatrix} \boldsymbol{B}_{c1} \\ \boldsymbol{B}_{c2} \end{bmatrix} \Delta \boldsymbol{\omega}$$

$$\begin{bmatrix} \Delta \boldsymbol{P}_m \\ \Delta \boldsymbol{U}_{PSS} \end{bmatrix} = \begin{bmatrix} \boldsymbol{J}_{31} & \boldsymbol{J}_{32} \\ \boldsymbol{J}_{41} & \boldsymbol{J}_{42} \end{bmatrix} \begin{bmatrix} \Delta \boldsymbol{X}_c \\ \Delta \boldsymbol{Y}_c \end{bmatrix} + \begin{bmatrix} \boldsymbol{B}_{c3} \\ \boldsymbol{B}_{c4} \end{bmatrix} \Delta \boldsymbol{\omega} \quad (1)$$

where $\Delta \boldsymbol{X}_c$ represents the state variables of controllers, $\Delta \boldsymbol{Y}_c$ represents the algebraic variables of controllers, $\Delta \boldsymbol{\omega}$ represents the rotor speed of the synchronous machines in which the controllers are installed, $\Delta \boldsymbol{P}_m$ and $\Delta \boldsymbol{U}_{PSS}$ are the output signals of the GTSs and PSSs respectively. The readers are referred to [1] for details on the frequency-domain model of power system stabilizers and governor-turbines.

After eliminating $\Delta \boldsymbol{Y}_c$, we have

$$s\Delta \boldsymbol{X}_c = \boldsymbol{A}_c \Delta \boldsymbol{X}_c + \boldsymbol{B}_c \Delta \boldsymbol{\omega}$$
$$\begin{bmatrix} \Delta \boldsymbol{P}_m \\ \Delta \boldsymbol{U}_{PSS} \end{bmatrix} = \boldsymbol{C}_c \Delta \boldsymbol{X}_c + \boldsymbol{D}_c \Delta \boldsymbol{\omega} \quad (2)$$

where

$$\boldsymbol{A}_c = \begin{bmatrix} \boldsymbol{J}_{11} - \boldsymbol{J}_{12}\boldsymbol{J}_{22}^{-1}\boldsymbol{J}_{21} \end{bmatrix}, \quad \boldsymbol{B}_c = \begin{bmatrix} \boldsymbol{B}_{c1} - \boldsymbol{J}_{12}\boldsymbol{J}_{22}^{-1}\boldsymbol{B}_{c2} \end{bmatrix}$$
$$\boldsymbol{C}_c = \begin{bmatrix} \boldsymbol{J}_{31} - \boldsymbol{J}_{32}\boldsymbol{J}_{22}^{-1}\boldsymbol{J}_{21} \\ \boldsymbol{J}_{41} - \boldsymbol{J}_{42}\boldsymbol{J}_{22}^{-1}\boldsymbol{J}_{21} \end{bmatrix}, \quad \boldsymbol{D}_c = \begin{bmatrix} \boldsymbol{B}_{c3} - \boldsymbol{J}_{32}\boldsymbol{J}_{22}^{-1}\boldsymbol{B}_{c2} \\ \boldsymbol{B}_{c4} - \boldsymbol{J}_{42}\boldsymbol{J}_{22}^{-1}\boldsymbol{B}_{c2} \end{bmatrix}$$
$$(3)$$

Then we have

$$\begin{bmatrix} \Delta \boldsymbol{P}_m \\ \Delta \boldsymbol{U}_{PSS} \end{bmatrix} = \begin{bmatrix} \boldsymbol{C}_c(s\boldsymbol{I} - \boldsymbol{A}_c)^{-1}\boldsymbol{B}_c + \boldsymbol{D}_c \end{bmatrix} \Delta \boldsymbol{\omega}$$
$$= \begin{bmatrix} \boldsymbol{G}_M(s) \\ \boldsymbol{H}_{PSS}(s) \end{bmatrix} \Delta \boldsymbol{\omega}$$
$$= \boldsymbol{T}(s)\Delta \boldsymbol{\omega} \quad (4)$$

where

$$\Delta\boldsymbol{\omega} = \begin{bmatrix} \Delta\omega_1 & \cdots & \Delta\omega_n \end{bmatrix}^T,$$

$$\Delta\boldsymbol{P}_m = \begin{bmatrix} \Delta P_{m,1} & \cdots & \Delta P_{m,n} \end{bmatrix}^T$$

$$\Delta\boldsymbol{U}_{PSS} = \begin{bmatrix} \Delta U_{PSS,1} & \cdots & \Delta U_{PSS,n} \end{bmatrix}^T \quad (5)$$

$$\boldsymbol{G}_M(s) = \begin{bmatrix} G_{M,1}(s) & & \\ & \ddots & \\ & & G_{M,n}(s) \end{bmatrix} \quad (6)$$

$$\boldsymbol{H}_{PSS}(s) = \begin{bmatrix} H_{PSS,1}(s) & & \\ & \ddots & \\ & & H_{PSS,n}(s) \end{bmatrix} \quad (7)$$

Here $G_{M,i}(s)$ and $H_{PSS,i}(s)$ are the transfer functions of the GTS and PSS installed in the $i$-th synchronous machine respectively, and $n$ is the number of synchronous machines in the power system.

The standard model of a synchronous machine is described as follows:

$$s\delta = \omega - \omega_b$$
$$M \cdot s\omega = P_m - P_e - K_D(\omega - \omega_b)$$
$$T'_{d0} \cdot sE'_q = -E'_q - (X_d - X'_d)I_d + E_{fd}$$
$$T_A \cdot sE_{fd} = -E_{fd} + K_A(U_t^* - U_t + U_{PSS})$$
$$0 = U_t \sin(\delta - \theta_t) - X_q I_q$$
$$0 = E'_q - U_t \cos(\delta - \theta_t) - X'_d I_d \quad (8)$$

As for the injection bus of each synchronous machine, we have

$$0 = I_d U_t \sin(\delta - \theta_t) + I_q U_t \cos(\delta - \theta_t) + P_{Lt}$$
$$- \sum_{j=1}^{n} U_t U_j Y_{tj} \cos(\theta_t - \theta_j - \alpha_{tj})$$
$$0 = I_d U_t \cos(\delta - \theta_t) - I_q U_t \sin(\delta - \theta_t) + Q_{Lt}$$
$$- \sum_{j=1}^{n} U_t U_j Y_{tj} \sin(\theta_t - \theta_j - \alpha_{tj}) \quad (9)$$

The definitions of the variables in (8) and (9) are explained in [9], [30], and [31].

The linearized state space model of the rest of the power system can be represented as follows:

$$\begin{bmatrix} s\Delta\boldsymbol{X}_g \\ 0 \end{bmatrix} = \begin{bmatrix} \boldsymbol{\Psi}_{11} & \boldsymbol{\Psi}_{12} \\ \boldsymbol{\Psi}_{21} & \boldsymbol{\Psi}_{22} \end{bmatrix} \begin{bmatrix} \Delta\boldsymbol{X}_g \\ \Delta\boldsymbol{Y}_g \end{bmatrix} + \begin{bmatrix} \boldsymbol{B}_{g1} & \boldsymbol{B}_{g2} \\ 0 & 0 \end{bmatrix} \begin{bmatrix} \Delta\boldsymbol{P}_m \\ \Delta\boldsymbol{U}_{PSS} \end{bmatrix}$$

$$\Delta\boldsymbol{\omega} = \begin{bmatrix} \boldsymbol{\Psi}_{31} & 0 \end{bmatrix} \begin{bmatrix} \Delta\boldsymbol{X}_g \\ \Delta\boldsymbol{Y}_g \end{bmatrix} \quad (10)$$

where $\Delta\boldsymbol{X}_g$ represents the state variables of the rest of the power system, $\Delta\boldsymbol{Y}_g$ represents the algebraic variables of the rest of the power system.

After eliminating $\Delta\boldsymbol{Y}_g$:

$$s\Delta\boldsymbol{X}_g = \boldsymbol{A}_g \Delta\boldsymbol{X}_g + \boldsymbol{B}_g \begin{bmatrix} \Delta\boldsymbol{P}_m \\ \Delta\boldsymbol{U}_{PSS} \end{bmatrix}$$

$$\Delta\boldsymbol{\omega} = \boldsymbol{C}_g \Delta\boldsymbol{X}_g + \boldsymbol{D}_g \begin{bmatrix} \Delta\boldsymbol{P}_m \\ \Delta\boldsymbol{U}_{PSS} \end{bmatrix} \quad (11)$$



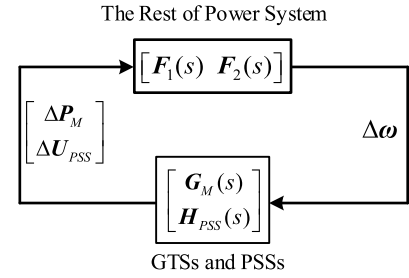**FIGURE 1.** The feedback interconnection model of the power system with the installation of GTSs and PSSs.

where

$$\boldsymbol{A}_g = \begin{bmatrix} \boldsymbol{\Psi}_{11} - \boldsymbol{\Psi}_{12}\boldsymbol{\Psi}_{22}^{-1}\boldsymbol{\Psi}_{21} \end{bmatrix}, \quad \boldsymbol{B}_g = \begin{bmatrix} \boldsymbol{B}_{g1} & \boldsymbol{B}_{g2} \end{bmatrix}$$
$$\boldsymbol{C}_g = [\boldsymbol{\Psi}_{31}], \quad \boldsymbol{D}_g = [0] \quad (12)$$

It can be derived that

$$\Delta\boldsymbol{\omega} = \begin{bmatrix} \boldsymbol{C}_G(s\boldsymbol{I} - \boldsymbol{A}_G)^{-1}\boldsymbol{B}_G + \boldsymbol{D}_G \end{bmatrix} \begin{bmatrix} \Delta\boldsymbol{P}_m \\ \Delta\boldsymbol{U}_{PSS} \end{bmatrix}$$

$$= \begin{bmatrix} \boldsymbol{F}_1(s) & \boldsymbol{F}_2(s) \end{bmatrix} \begin{bmatrix} \Delta\boldsymbol{P}_m \\ \Delta\boldsymbol{U}_{PSS} \end{bmatrix}$$

$$= \boldsymbol{F}(s) \begin{bmatrix} \Delta\boldsymbol{P}_m \\ \Delta\boldsymbol{U}_{PSS} \end{bmatrix} \quad (13)$$

where

$$\boldsymbol{F}_1(s) = \begin{bmatrix} F_{1,1}(s) & \cdots & F_{1,n}(s) \\ \vdots & \ddots & \vdots \\ F_{n,1}(s) & \cdots & F_{n,n}(s) \end{bmatrix},$$

$$\boldsymbol{F}_2(s) = \begin{bmatrix} F_{1,n+1}(s) & \cdots & F_{1,2n}(s) \\ \vdots & \ddots & \vdots \\ F_{n,n+1}(s) & \cdots & F_{n,2n}(s) \end{bmatrix} \quad (14)$$

According to (4) and (13), the feedback interconnection model of the power system with the installation of GTSs and PSSs can be presented in the form as Fig. 1 depicts.

### B. THE FEEDBACK INTERCONNECTION MODEL OF POWER SYSTEMS INTEGRATED WITH WIND TURBINE GENERATORS

Taking the voltage amplitude of the interconnection nodes between WTGs and power system as the input signals and the power output of WTGs as the output signals, the linearized state-space model of the WTGs can be demonstrated as follows:

$$\begin{bmatrix} s\Delta\boldsymbol{X}_w \\ 0 \end{bmatrix} = \begin{bmatrix} \boldsymbol{\Gamma}_{11} & \boldsymbol{\Gamma}_{12} \\ \boldsymbol{\Gamma}_{21} & \boldsymbol{\Gamma}_{22} \end{bmatrix} \begin{bmatrix} \Delta\boldsymbol{X}_w \\ \Delta\boldsymbol{Y}_w \end{bmatrix} + \begin{bmatrix} \boldsymbol{B}_{w1} \\ \boldsymbol{B}_{w2} \end{bmatrix} \Delta\boldsymbol{U}_w$$

$$\begin{bmatrix} \Delta\boldsymbol{P}_w \\ \Delta\boldsymbol{Q}_w \end{bmatrix} = \begin{bmatrix} 0 & \boldsymbol{\Gamma}_{32} \\ 0 & \boldsymbol{\Gamma}_{42} \end{bmatrix} \begin{bmatrix} \Delta\boldsymbol{X}_w \\ \Delta\boldsymbol{Y}_w \end{bmatrix} + \begin{bmatrix} \boldsymbol{B}_{w3} \\ \boldsymbol{B}_{w4} \end{bmatrix} \Delta\boldsymbol{U}_w \quad (15)$$

where $\Delta\boldsymbol{X}_w$ represents the state variables of WTGs, $\Delta\boldsymbol{Y}_w$ represents the algebraic variables of WTGs, $\Delta\boldsymbol{U}_w$ represents the voltage amplitude of the interconnection nodes, $\Delta\boldsymbol{P}_w$ and $\Delta\boldsymbol{Q}_w$ are the active and reactive power of WTGs.

After eliminating $\Delta Y_w$, we have

$$s\Delta X_w = A_w \Delta X_w + B_w \Delta U_w$$
$$\begin{bmatrix} \Delta P_w \\ \Delta Q_w \end{bmatrix} = C_w \Delta X_w + D_w \Delta U_w \tag{16}$$

where

$$A_w = \left[ \Gamma_{11} - \Gamma_{12}\Gamma_{22}^{-1}\Gamma_{21} \right], \quad B_w = \left[ B_{w1} - \Gamma_{12}\Gamma_{22}^{-1}B_{w2} \right],$$
$$C_w = \begin{bmatrix} -\Gamma_{32}\Gamma_{22}^{-1}\Gamma_{21} \\ -\Gamma_{42}\Gamma_{22}^{-1}\Gamma_{21} \end{bmatrix}, \quad D_w = \begin{bmatrix} B_{w3} - \Gamma_{32}\Gamma_{22}^{-1}\Gamma_{21}B_{w2} \\ B_{w4} - \Gamma_{42}\Gamma_{22}^{-1}\Gamma_{21}B_{w2} \end{bmatrix} \tag{17}$$

Then the transfer function matrix of WTGs is:

$$\begin{aligned} \begin{bmatrix} \Delta P_w \\ \Delta Q_w \end{bmatrix} &= \left[ C_w (sI - A_w)^{-1} B_w + D_w \right] \Delta U_w \\ &= \begin{bmatrix} W_P(s) \\ W_Q(s) \end{bmatrix} \Delta U_w \\ &= W(s)\Delta U_w \end{aligned} \tag{18}$$

where

$$\Delta P_w = \begin{bmatrix} \Delta P_{w,1} & \cdots & \Delta P_{w,n} \end{bmatrix}^T,$$
$$\Delta Q_w = \begin{bmatrix} \Delta Q_{w,1} & \cdots & \Delta Q_{w,n} \end{bmatrix}^T$$
$$\Delta U_w = \begin{bmatrix} \Delta U_{w,1} & \cdots & \Delta U_{w,n} \end{bmatrix}^T \tag{19}$$

$$W_P(s) = \begin{bmatrix} W_{P,1}(s) & & \\ & \ddots & \\ & & W_{P,m}(s) \end{bmatrix},$$

$$W_Q(s) = \begin{bmatrix} W_{Q,1}(s) & & \\ & \ddots & \\ & & W_{Q,m}(s) \end{bmatrix} \tag{20}$$

$m$ is the number of WTGs integrated in the power system.

Refer to (8) and (9), the linearized state space model of the synchronous machines in the power system is shown as follows:

$$\begin{bmatrix} s\Delta X_G \\ 0 \end{bmatrix} = \begin{bmatrix} \Phi_{11} & \Phi_{12} \\ \Phi_{21} & \Phi_{22} \end{bmatrix} \begin{bmatrix} \Delta X_G \\ \Delta Y_G \end{bmatrix} \tag{21}$$

where $\Delta X_G$ represents the state variables of the rest of the power system, $\Delta Y_G$ represents the algebraic variables of the rest of the power system.

As for the injection bus of each WTG, we have

$$0 = P_w - \sum_{j=1}^{n} U_w U_j Y_{wj} \cos(\theta_w - \theta_j - \alpha_{wj})$$

$$0 = Q_w - \sum_{j=1}^{n} U_w U_j Y_{wj} \sin(\theta_w - \theta_j - \alpha_{wj}) \tag{22}$$

where $U_w$ and $\theta_w$ are the voltage amplitude and phase-angle of the injection bus of WTG, $U_j$ and $\theta_j$ are the voltage amplitude and phase-angle of the $j$-th bus of the system, $Y_{wj}$ and $\alpha_{wj}$ are the amplitude and phase-angle of admittance between the injection bus of WTG and bus $j$.

After linearizing (22) for all the WTG buses in the system and combined with (21), the linearized state space model of the rest of the power system can be expressed as:

$$\begin{bmatrix} s\Delta X_G \\ 0 \\ 0 \end{bmatrix} = \begin{bmatrix} \Phi_{11} & \Phi_{12} \\ \Phi_{21} & \Phi_{22} \\ 0 & \Phi_{32} \end{bmatrix} \begin{bmatrix} \Delta X_G \\ \Delta Y_G \end{bmatrix} + \begin{bmatrix} 0 \\ 0 \\ B_{G3} \end{bmatrix} \begin{bmatrix} \Delta P_w \\ \Delta Q_w \end{bmatrix}$$

$$\Delta U_w = \begin{bmatrix} 0 & \Phi_{42} \end{bmatrix} \begin{bmatrix} \Delta X_G \\ \Delta Y_G \end{bmatrix} \tag{23}$$

After eliminating $\Delta Y_G$, we have

$$s\Delta X_G = A_G \Delta X_G + B_G \begin{bmatrix} \Delta P_w \\ \Delta Q_w \end{bmatrix}$$

$$\Delta U_w = C_G \Delta X_G + D_G \begin{bmatrix} \Delta P_w \\ \Delta Q_w \end{bmatrix} \tag{24}$$

where

$$A_G = \left[ \Phi_{11} - \Phi_{12} \begin{bmatrix} \Phi_{22} \\ \Phi_{32} \end{bmatrix}^{-1} \begin{bmatrix} \Phi_{21} \\ 0 \end{bmatrix} \right],$$

$$B_G = \left[ -\Phi_{12} \begin{bmatrix} \Phi_{22} \\ \Phi_{32} \end{bmatrix}^{-1} \begin{bmatrix} 0 \\ B_{G3} \end{bmatrix} \right],$$

$$C_G = \left[ -\Phi_{42} \begin{bmatrix} \Phi_{22} \\ \Phi_{32} \end{bmatrix}^{-1} \begin{bmatrix} \Phi_{21} \\ 0 \end{bmatrix} \right],$$

$$D_G = \left[ -\Phi_{42} \begin{bmatrix} \Phi_{22} \\ \Phi_{32} \end{bmatrix}^{-1} \begin{bmatrix} 0 \\ B_{G3} \end{bmatrix} \right] \tag{25}$$

Then the transfer function matrix of the rest of the power system can be derived as:

$$\begin{aligned} \Delta U_w &= \left[ C_G (sI - A_G)^{-1} B_G + D_G \right] \begin{bmatrix} \Delta P_w \\ \Delta Q_w \end{bmatrix} \\ &= \begin{bmatrix} G_P(s) & G_Q(s) \end{bmatrix} \begin{bmatrix} \Delta P_w \\ \Delta Q_w \end{bmatrix} \\ &= G(s) \begin{bmatrix} \Delta P_w \\ \Delta Q_w \end{bmatrix} \end{aligned} \tag{26}$$

where

$$G_P(s) = \begin{bmatrix} G_P^{1-1}(s) & \cdots & G_P^{1-m}(s) \\ \vdots & \ddots & \vdots \\ G_P^{m-1}(s) & \cdots & G_P^{m-m}(s) \end{bmatrix} \tag{27}$$

$$G_Q(s) = \begin{bmatrix} G_Q^{1-1}(s) & \cdots & G_Q^{1-m}(s) \\ \vdots & \ddots & \vdots \\ G_Q^{m-1}(s) & \cdots & G_Q^{m-m}(s) \end{bmatrix} \tag{28}$$

Similarly, the feedback interconnection model of the power system with the integration of WTGs can be displayed in Fig. 2.

## III. PROPOSED METHODOLOGY

In this section, on the basis of the afore-mentioned feedback interconnection models, a new methodology is proposed to analyze the impact of GTSs, PSSs and WTGs on small-disturbance stability.
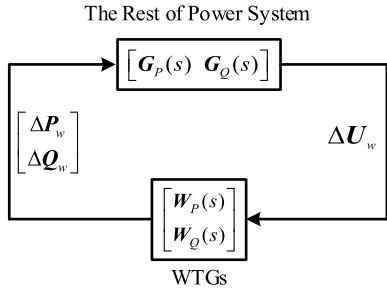
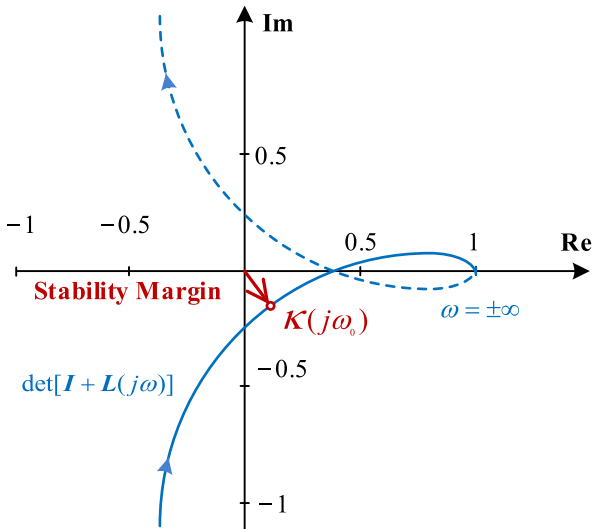**FIGURE 2.** The feedback interconnection model of the power system with the integration of WTGs.



**FIGURE 4.** The definition of dividing line.



**FIGURE 3.** Nyquist Curve And Stability Margin.

## A. STABILITY MARGIN BASED ON THE GENERALIZED NYQUIST CRITIRION

First we briefly review the celebrated generalized Nyquist theorem for multi-input multi-output system [32]. Let $\rho_0$ be the number of open-loop unstable poles, then the closed-loop system with loop transfer function matrix $L(s)$ is stable if and only if the Nyquist curve of $\det[I + L(s)]$

(1) makes $\rho_0$ anti-clockwise encirclements of the origin;
(2) does not pass through the origin.

In general, $\rho_0$ of a power system is equal to 0, therefore, the minimum distance between the origin and the Nyquist curve of $\det[I + L(s)]$ can be regarded as the stability margin of the closed-loop system (see Fig. 3) [33], [34]. Furthermore, the frequency corresponding to the point closest to the origin on the Nyquist curve is typically near the frequency of the low-frequency oscillation mode with weak damping (denoted as $\omega_0$), hence it is more efficient to acquire the stability margin by calculating $\det[I + L(j\omega_0)]$ instead of sweeping frequencies. For convenience, let us denote $\kappa(j\omega_0)$ as the point on the Nyquist curve closest to the origin in the subsequent sections.
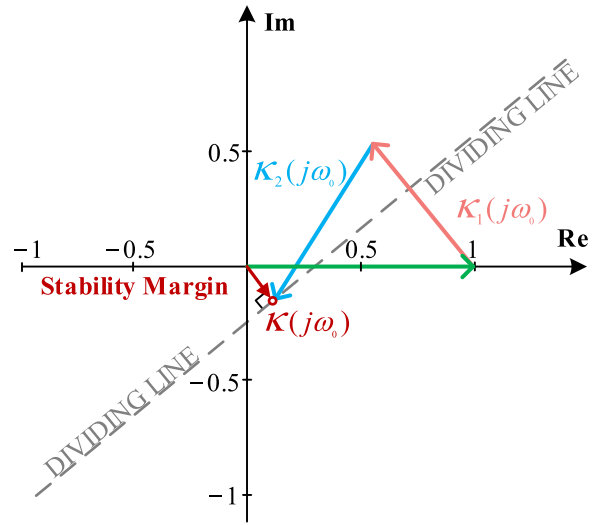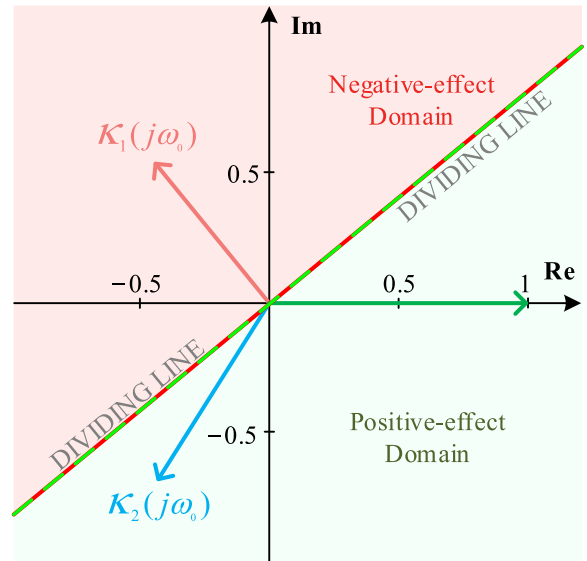


**FIGURE 5.** The definitions of Positive-effect domain and negative-effect domain.

## B. THE IMPACT OF CONTROLLERS AND WIND TURBINE GENERATORS ON STABILITY MARGIN

For a power system with a GTS and a PSS, the critical point $\kappa(j\omega_0)$ can be represented as:

$$
\begin{aligned}
\kappa(j\omega_0) &= \det\left[I - L(j\omega_0)\right] \\
&= 1 - \begin{bmatrix} F_1(j\omega_0) & F_2(j\omega_0) \end{bmatrix} \begin{bmatrix} G_M(j\omega_0) \\ H_{PSS}(j\omega_0) \end{bmatrix} \\
&= 1 \underbrace{-F_1(j\omega_0)G_M(j\omega_0)}_{\kappa_1(j\omega_0)} \underbrace{-F_2(j\omega_0)H_{PSS}(j\omega_0)}_{\kappa_2(j\omega_0)} \\
&= 1 + \kappa_1(j\omega_0) + \kappa_2(j\omega_0)
\end{aligned}
\tag{29}
$$

From (29), the impact of the GTS and PSS on stability margin can be conveniently identified through $\kappa_1(j\omega_0)$ and $\kappa_2(j\omega_0)$, which is a Nyquist-type result. An illustrative

example is provided in Fig. 4. The line perpendicular to the line connecting $\kappa(j\omega_0)$ and the origin can be viewed as a dividing line. Fig. 5 further provides an explanation. The starting points of $\kappa_1(j\omega_0)$ and $\kappa_2(j\omega_0)$ are moved to the origin, it is manifest that $\kappa_1(j\omega_0)$ moves $\kappa(j\omega_0)$ closer to the origin, reducing the stability margin, while $\kappa_2(j\omega_0)$ moves $\kappa(j\omega_0)$ away from the origin, which increases the stability domain. In this way, the positive-effect domain and negative-effect domain in the complex plane can be clearly divided, which are demonstrated in Fig. 5.

When a power system is installed with multiple GTSs and PSSs, the expression of $\kappa(j\omega_0)$ is more complicated since $L(j\omega_0)$ becomes a matrix and $\kappa(j\omega_0)$ cannot be transformed into the sum of several vectors directly. This is precisely why it is in general difficult to perform stability analysis for a multi-input multi-output system.

A key finding of the present work is to be able to recognize that the rank of $L(j\omega_0)$ is approximately equal to 1, using this property can greatly simplify the expression of the det$[I - L(j\omega_0)]$ for a multi-input multi-output system, resolving the above-mentioned challenge. This enables us to conveniently perform stability study in a Nyquist fashion as equation (29) does. The proof is shown in Appendix. Combined with the fact that $rank[F(j\omega_0)T(j\omega_0)] \approx 1$, we have

$$
\begin{aligned}
\kappa&(j\omega_0) \\
&= \det\left[I - L(j\omega_0)\right] \\
&= \det\left[I - F(j\omega_0)T(j\omega_0)\right] \\
&\approx 1 - L_{1,1}(j\omega_0) - L_{2,2}(j\omega_0) - \cdots L_{n,n}(j\omega_0) \\
&= 1 - \underbrace{[F_{1,1}(j\omega_0)G_{M,1}(j\omega_0) + F_{1,n+1}(j\omega_0)H_{PSS,1}(j\omega_0)]}_{L_{1,1}(j\omega_0)} \\
&\quad - \cdots -\underbrace{[F_{n,n}(j\omega_0)G_{M,n}(j\omega_0) + F_{n,2n}(j\omega_0)H_{PSS,n}(j\omega_0)]}_{L_{n,n}(j\omega_0)} \\
&= 1 \underbrace{-F_{1,1}(j\omega_0)G_{M,1}(j\omega_0) - \cdots - F_{n,n}(j\omega_0)G_{M,n}(j\omega_0)}_{\text{The impact of all the GTSs}} \\
&\quad \underbrace{-F_{1,n+1}(j\omega_0)H_{PSS,1}(j\omega_0) - \cdots - F_{n,2n}(j\omega_0)H_{PSS,n}(j\omega_0)}_{\text{The impact of all the PSSs}}
\end{aligned}
$$

(30)

It can be seen from (30) that $\kappa(j\omega_0)$ is again expressed as the sum of vectors, which has the same form as in (29). The above formula can be conveniently used to quantify the impact of GTSs and PSSs on stability margin.

Moreover, the parameters of GTSs and PSSs can also be optimized in light of the above result. For instance, the impact of the first PSS is determined by $-F_{1,n+1}(j\omega_0)H_{PSS,1}(j\omega_0)$, if the calculation result shows that the PSS exerts negative effect on stability margin, then the phase of $-F_{1,n+1}(j\omega_0)H_{PSS,1}(j\omega_0)$ can be adjusted through tuning the parameters of $H_{PSS,1}(j\omega_0)$, so that the effect of the PSS can be fine-tuned. A more specific example is provided in next section to verify the effectiveness of the method.

As for the feedback interconnection model of the power system with the integration of multiple WTGs, the expression
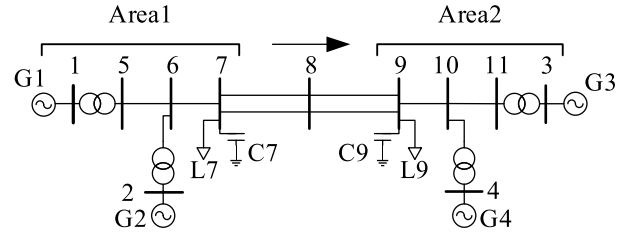


**FIGURE 6. Four-machine two-area system.**

**TABLE 1. Parameters of PSSs in initial case.**

| Parameters | PSS$_1$ | PSS$_2$ | PSS$_3$ | PSS$_4$ |
|---|---|---|---|---|
| K | 0.2 | 0.2 | 0.2 | 0.2 |
| T$_a$ | 0.01 | 0.503 | 1.2 | 0.4 |
| T$_b$ | 0.03 | 0.03 | 0.03 | 0.03 |

**TABLE 2. Parameters of GTSs in initial case.**

| Parameters | GTS$_1$ | GTS$_2$ | GTS$_3$ | GTS$_4$ |
|---|---|---|---|---|
| R | 0.05 | 0.05 | 0.05 | 0.05 |
| T$_G$ | 0.2 | 0.2 | 0.2 | 0.2 |
| T$_{CH}$ | 0.3 | 0.3 | 0.3 | 0.3 |

of $\kappa(j\omega_0)$ is as follows:

$$
\begin{aligned}
\kappa(j\omega_0) &= \det\left[I - L(j\omega_0)\right] \\
&= \det\left[I - G(j\omega_0)W(j\omega_0)\right] \\
&\approx 1 - L_{1,1}(j\omega_0) - L_{2,2}(j\omega_0) - \cdots L_{m,m}(j\omega_0) \\
&= 1 - \underbrace{[G_P^{1-1}W_{P,1}(j\omega_0) + G_Q^{1-1}W_{Q,1}(j\omega_0)]}_{The\text{impact of the first WTG}} \\
&\quad - \cdots - \underbrace{[G_P^{m-m}W_{P,m}(j\omega_0) + G_Q^{m-m}W_{Q,m}(j\omega_0)]}_{The\text{impact of the m-th WTG}}
\end{aligned}
$$

(31)

Likewise, the vectors above indicate readily the contribution of each WTG to the small-disturbance stability margin.

## IV. CASE STUDY

In this section, two cases are presented to validate the efficacy of the proposed method. The impact of GTSs and PSSs on small-disturbance stability margin for four-machine two-area system is demonstrated firstly, then the parameter optimization on the basis of the introduced results is performed. The data of a regional power grid in China is utilized to examine the impact of WTGs on small-disturbance stability margin. The conclusions drawn by the suggested method are verified through eigenvalue calculation.

### A. FOUR-MACHINE TWO-AREA SYSTEM

The configuration of four-machine two-area power system is shown in Fig. 6. Parameters of the system are given in [1]. GTS$_1$-GTS$_4$ and PSS$_1$-PSS$_4$ are installed in generators
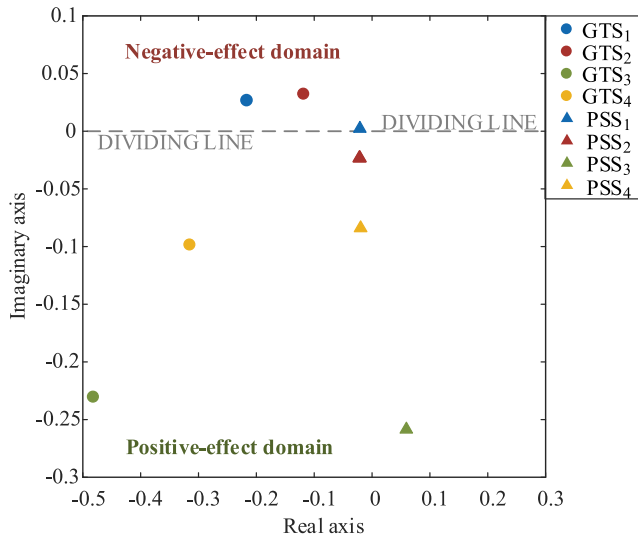
**FIGURE 7.** The impact of GTSs and PSSs in initial case.

**TABLE 3. Inter-area mode in 9 cases.**

| Case | Real part | Imaginary part | Damping ratio (%) | Frequency (Hz) |
|---|---|---|---|---|
| Initial | −0.0254 | 3.6287 | 0.70— | 0.58 |
| **1** | **−0.0275** | **3.6239** | **0.76 ↑** | **0.58** |
| **2** | **−0.0278** | **3.6199** | **0.77 ↑** | **0.58** |
| 3 | −0.0179 | 3.6072 | 0.50 ↓ | 0.57 |
| 4 | −0.0224 | 3.6147 | 0.62 ↓ | 0.58 |
| **5** | **−0.0256** | **3.6278** | **0.71 ↑** | **0.58** |
| 6 | −0.0246 | 3.6276 | 0.68 ↓ | 0.58 |
| 7 | −0.0145 | 3.6299 | 0.40 ↓ | 0.58 |
| 8 | −0.0220 | 3.6275 | 0.61 ↓ | 0.58 |

G1-G4 respectively. The transfer functions of GTSs and PSSs are provided in (32) below [35], [36], and the initial parameters are provided in Table 1 and Table 2. It is worth mentioning that the initial parameters are designed intentionally to facilitate the presentation of the proposed method. Area

$$G_M(s) = \frac{\Delta P_M}{\Delta \omega} = -\frac{1}{R} \cdot \frac{1}{1 + sT_G} \cdot \frac{1}{1 + sT_{CH}}$$

$$H_{PSS}(s) = \frac{\Delta U_{PSS}}{\Delta \omega} = \frac{K(1 + sT_a)}{(1 + sT_b)} \tag{32}$$

The inter-area oscillation mode of the system is $\lambda_0 = -0.0254 + 3.6287j$, the corresponding damping ratio is 0.7%. Substituting $s = 3.6287j$ into (30), we obtained the singular values of matrix $\boldsymbol{F}(j\omega_0)\boldsymbol{T}(j\omega_0)$ as

$$[0.95146, 0.00103, 0.00069, 0.00050].$$

This is an excellent evidence for the assertion that the rank of matrix $\boldsymbol{F}(j\omega_0)\boldsymbol{T}(j\omega_0)$ is close to 1.

The impact of $GTS_1$-$GTS_4$ and $PSS_1$-$PSS_4$ is displayed in Fig. 7. In this case, the point closest to the origin on the Nyquist curve is $-0.1410 - 0.6282j$, and $\kappa(j\omega_0) = -0.1334 - 0.6342j$, which is close to the imaginary axis, thus

**TABLE 4. Phase of vectors.**

| Vectors | Phase | | |
|---|---|---|---|
| $-F_{1,1} / -F_{2,2} / -F_{1,5}$ | 75.5337° | 67.1973° | 177.1796° |
| $G_{M,1} / G_{M,2} / H_{PSS,1}$ | 96.580° | 96.580° | −4.136° |
| Total | 172.114° | 163.778° | 173.043° |

**TABLE 5. Optimized parameters of controllers.**

| Cases | Optimized parameters |
|---|---|
| 9 | $T_{a1}$=0.609 |
| 10 | $T_{a1}$=0.609, $T_{G1}$=0.1 |
| 11 | $T_{a1}$=0.609, $T_{G1}$=0.1, $T_{G2}$=0.08 |

**TABLE 6. Inter-area mode in 4 cases.**

| Case | Real part | Imaginary part | Damping ratio (%) | Frequency (Hz) |
|---|---|---|---|---|
| Initial | −0.025 | 3.6287 | 0.70 | 0.58 |
| 9 | −0.027 | 3.6293 | 0.75 | 0.58 |
| 10 | −0.030 | 3.6311 | 0.82 | 0.58 |
| 11 | −0.031 | 3.6324 | 0.87 | 0.58 |

the real axis can be regarded as the dividing line. The positive-effect domain and negative-effect domain are also marked in the figure.

It is evident that $GTS_1$, $GTS_2$ and $PSS_1$ have negative effect while the other GTSs and PSSs have positive effect on system stability. The inter-area oscillation mode is calculated in different cases to prove the conclusion above and the results are listed in Table 3, where Case1-Case4 respectively correspond to $GTS_1$-$GTS_4$ being out of service, and Case5-Case8 respectively correspond to $PSS_1$-$PSS_4$ being out of service.

From Table 3, it can be seen that the damping ratio of the inter-area mode increases when $GTS_1$, $GTS_2$ and $PSS_1$ are out of service, in other cases, the damping ratio drops to varying degrees. The results verifies that $GTS_1$, $GTS_2$ and $PSS_1$ worsened the stability, while the other controllers enhance the stability of the system, which is highly consistent with the conclusion drawn by the proposed method.

Using the proposed method, the negative effect of $GTS_1$, $GTS_2$ and $PSS_1$ can be reversed by parameter tuning. According to (30), $\kappa(j\omega_0)$ can be expressed as:

$$\kappa(j\omega_0) = 1 - F_{1,1}(j\omega_0)G_{M,1}(j\omega_0) - F_{2,2}(j\omega_0)G_{M,2}(j\omega_0)$$
$$- F_{3,3}(j\omega_0)G_{M,3}(j\omega_0) - F_{4,4}(j\omega_0)G_{M,4}(j\omega_0)$$
$$- F_{1,5}(j\omega_0)H_{PSS,1}(j\omega_0) - F_{2,6}(j\omega_0)H_{PSS,2}(j\omega_0)$$
$$- F_{3,7}(j\omega_0)H_{PSS,3}(j\omega_0) - F_{4,8}(j\omega_0)H_{PSS,4}(j\omega_0) \tag{33}$$

The phase of the vectors corresponding to $GTS_1$, $GTS_2$ and $PSS_1$ are demonstrated in Table 4. The phase of $-F_{1,1}(j\omega_0)$, $-F_{2,2}(j\omega_0)$ and $-F_{1,5}(j\omega_0)$ is less than 180°, the parameters of controllers can be designed to shift
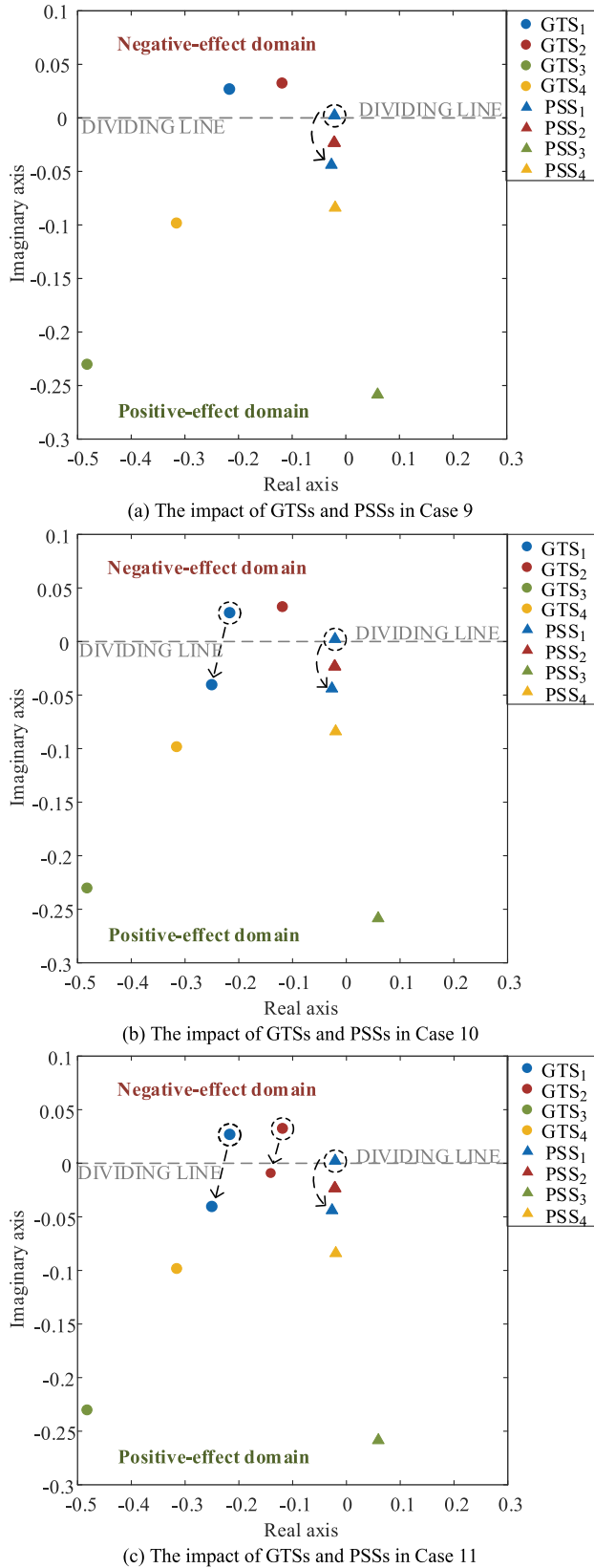
(a) The impact of GTSs and PSSs in Case 9



(b) The impact of GTSs and PSSs in Case 10



(c) The impact of GTSs and PSSs in Case 11

**FIGURE 8.** The impact of GTSs and PSSs in Case 9-11.

**TABLE 7.** Areas and names of injected buses of WTGs.

| Areas | Names of buses | |
|---|---|---|
| J | J1 | J2 |
| M | M1 | M2 |
| S | S1 | S2 |
| X | X1 | X2 |
| N | N1 | N2 |
| Z | Z1 | Z2 |
| H | H1 | H2 |

**TABLE 8.** Interarea mode in 15 cases.

| Case | Real part | Imaginary part | Damping ratio (%) | Frequency (Hz) |
|---|---|---|---|---|
| Initial | −0.15139 | 2.80449 | 5.3903 — | 0.4465 |
| J1 | −0.15164 | 2.80577 | 5.3967 ↑ | 0.4467 |
| J2 | −0.15162 | 2.80578 | 5.3960 ↑ | 0.4467 |
| M1 | −0.15152 | 2.80597 | 5.3921 ↑ | 0.4468 |
| M2 | −0.15152 | 2.80598 | 5.3920 ↑ | 0.4468 |
| S1 | −0.15181 | 2.80528 | 5.4037 ↑ | 0.4467 |
| S2 | −0.15178 | 2.80549 | 5.4022 ↑ | 0.4467 |
| X1 | −0.15213 | 2.80558 | 5.4145 ↑ | 0.4467 |
| X2 | −0.15217 | 2.80506 | 5.4169 ↑ | 0.4466 |
| N1 | −0.15178 | 2.80632 | 5.4006 ↑ | 0.4468 |
| **N2** | **−0.15145** | **2.80618** | **5.3892 ↓** | **0.4468** |
| Z1 | −0.15177 | 2.80616 | 5.4006 ↑ | 0.4468 |
| Z2 | −0.15159 | 2.80618 | 5.3941 ↑ | 0.4468 |
| H1 | −0.15154 | 2.80624 | 5.3923 ↑ | 0.4468 |
| H2 | −0.15174 | 2.80583 | 5.4001 ↑ | 0.4467 |

In accordance with the analysis above, the parameters of $PSS_1$, $GTS_1$ and $GTS_2$ are optimized in order in Case9-Case11. The tuned parameters are shown in Table 5. Other parameters remain unchanged.

The impact of the controllers in Case9-Case11 is depicted in Fig. 8. The vectors in circles correspond to the impact of controllers in the initial case, and the arrows show the impact of controllers after parameter optimization. Obviously, the impact of $PSS_1$, $GTS_1$ and $GTS_2$ has been reversed from negative to positive side. The results are further verified by the eigenvalues shown in Table 6.

### B. AN ACTUAL LARGE-SCALE POWER SYSTEM
In this example, the impact of WTGs on small-disturbance stability margin for a regional power grid in China is investigated. 14 WTGs whose power output is 49.5MW and 0MVar are selected from 7 areas in the system, and the names of the injection buses are listed in Table 7.

The inter-area mode under study is $\lambda_0 = -0.1514 + 2.8045j$, damping ratio is 5.390%. Substituting $s = 2.8045j$ into (31), we obtained the singular values of $G(j\omega_0)W(j\omega_0)$ as

[121.03412, 0.009832, 0.008348, 0.007356, 0.006233, 0.005420, 0.004911, 0.004871, 0.004665, 0.004316, 0.004058, 0.003851, 0.003732, 0.003601].

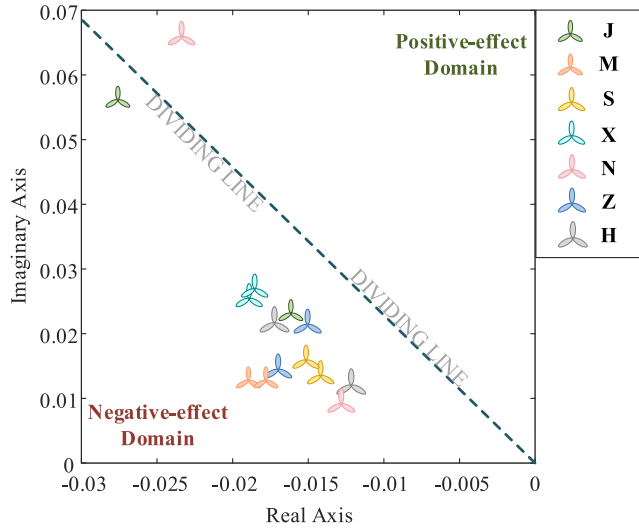Again, the singular values nicely verify the approximate rank-one property of matrix $G(j\omega_0)W(j\omega_0)$.

the phase of $-F_{1,1}(j\omega_0)G_{M,1}(j\omega_0)$, $-F_{2,2}(j\omega_0)G_{M,2}(j\omega_0)$ and $-F_{1,5}(j\omega_0)H_{PSS,1}(j\omega_0)$ to exceed 180°.

**FIGURE 9.** The impact of 14 WTGs on stability margin.

The impact of WTGs on stability margin is presented in Fig. 9. The point on the Nyquist curve closest to the origin in this case is $0.7491 + 0.3211\,j$, while $\kappa(j\omega_0)$ is equal to $0.7554 + 0.3304\,j$. The dividing line, the positive-effect domain and the negative-effect domain are also marked in the figure. It is clear that only 1 WTG have positive impact on stability, while the other 13 WTGs have negative effect on stability. The eigenvalue calculations are also performed to verify the results demonstrated in Fig. 9. Table 8 shows the inter-area mode after 14 WTGs are sequentially replaced with constant power source.

It can be seen that the damping ratio of the inter-area mode decreases when constant power source replaces the positive-effect WTG, which means N2 is beneficial to stability. The effectiveness of the new method is proved.

## V. CONCLUSION

This paper introduces a frequency-domain approach to evaluate the impact of GTSs, PSSs and WTGs on small-disturbance stability margin. The feedback interconnection model of power system with the installation of GTSs and PSSs and the feedback interconnection model of power system with the integration of WTGs are presented. It is found that the rank of the loop transfer function matrix at the low-frequency oscillation frequency is approximately equal to 1. Based on that and the generalized Nyquist criterion, the impact of GTSs, PSSs and WTGs on stability margin can be identified. Compared with other analysis approach, the proposed approach can avoid the calculation of eigenvalues, eigenvectors and residues, only simple matrix operations are required to analyze the impact of multiple controllers. Furthermore, the Nyquist-type analysis results can be employed to conveniently optimize the parameters of controllers.

## APPENDIX

In this appendix, the property that the rank of $\boldsymbol{L}(j\omega_0)$ is approximately equal to 1 is proved.

Notice that the transfer function matrix of the rest of the power system can be described as:

$$\boldsymbol{F}(s) = \begin{bmatrix} \dfrac{R_{1,1}^1}{s-\lambda_1} + \cdots \dfrac{R_{1,1}^k}{s-\lambda_k} & \cdots & \dfrac{R_{1,2n}^1}{s-\lambda_1} + \cdots \dfrac{R_{1,2n}^k}{s-\lambda_k} \\ \vdots & \ddots & \vdots \\ \dfrac{R_{n,1}^1}{s-\lambda_1} + \cdots \dfrac{R_{n,1}^k}{s-\lambda_k} & \cdots & \dfrac{R_{n,2n}^1}{s-\lambda_1} + \cdots \dfrac{R_{n,2n}^k}{s-\lambda_k} \end{bmatrix} \tag{34}$$

where $\lambda_1, \cdots, \lambda_k$ are the eigenvalues of the power system before the installation of controllers. Here $[R_{i,j}^x]$ are the residue matrix corresponding to the $x$-th eigenvalue and the rank of each $[R_{i,j}^x]$ is exactly equal to 1 [37], that is:

$$rank[R_{i,j}^x] = 1 \tag{35}$$

Assume that $\lambda_1$ is the weakly damped LFO mode. It is easy to know that $|j\omega_0 - \lambda_1|$ is much smaller than $|j\omega_0 - \lambda_x|$, for $x = 2, 3, \ldots, k$. It follows that

$$\left| \frac{R_{i,j}^1}{j\omega_0 - \lambda_1} \right| \gg \left| \frac{R_{i,j}^x}{j\omega_0 - \lambda_x} \right| \tag{36}$$

The above result immediately leads to the following observation

$$\boldsymbol{F}(j\omega_0) \approx \begin{bmatrix} \dfrac{R_{1,1}^1}{j\omega_0-\lambda_1} & \cdots & \dfrac{R_{1,2n}^1}{j\omega_0-\lambda_1} \\ \vdots & \ddots & \vdots \\ \dfrac{R_{n,1}^1}{j\omega_0-\lambda_1} & \cdots & \dfrac{R_{n,2n}^1}{j\omega_0-\lambda_1} \end{bmatrix} = \frac{\left[R_{i,j}^1\right]}{j\omega_0 - \lambda_1} \tag{37}$$

Since $rank[R_{i,j}^x] = 1$, it follows that

$$rank[\boldsymbol{F}(j\omega_0)] \approx 1 \tag{38}$$

*Theorem (Sylvester Inequality) [38]:* If the dimensions of the matrices $\mathbf{A}$ and $\mathbf{B}$ are $m \times k$ and $k \times n$ respectively, then

$$rank(\boldsymbol{A} \cdot \boldsymbol{B}) \leq \min(rank\boldsymbol{A}, rank\boldsymbol{B}). \tag{39}$$

According to the above result, we have:

$$rank[\boldsymbol{F}(j\omega_0)\boldsymbol{T}(j\omega_0)] \leq \min\{rank[\boldsymbol{F}(j\omega_0)], rank[\boldsymbol{T}(j\omega_0)]\} \tag{40}$$

An important consequence of the above equation is that

$$rank[\boldsymbol{F}(j\omega_0)\boldsymbol{T}(j\omega_0)] \approx 1. \tag{41}$$

Based on the above result, in what follows, we proceed to introduce the so-called *expansion for diagonal matrices* [39] to simply the expression of stability margin. We denote by $\boldsymbol{Y}_{i_1 \cdots i_k}$ the principal submatrix of order $n - k$ obtained by deleting rows and columns $i_1 \cdots i_k$ of the $n \times n$ matrix $\mathbf{Y}$. Let $\mathbf{Z}$ and $\mathbf{Y}$ be $n \times n$ complex matrices. If $\boldsymbol{Z} = diag(z_1 \cdots z_n)$, then

$$\det(\boldsymbol{Z} + \boldsymbol{Y}) = \det(\boldsymbol{Z}) + \det(\boldsymbol{Y}) + e_1 + \cdots + e_{n-1} \tag{42}$$

where

$$e_k \equiv \sum_{1 \le i_1 < \cdots < i_k \le n} z_{i1} \cdots z_{ik} \det(\boldsymbol{Y}_{i_1 \cdots i_k}), \ 1 \le k \le n-1$$

(43)

Then we can infer that

$$
\begin{aligned}
\kappa(j\omega_0) \\
= \det[\boldsymbol{I} - \boldsymbol{L}(j\omega_0)] \\
= \det[\boldsymbol{I} - \boldsymbol{F}(j\omega_0)\boldsymbol{T}(j\omega_0)] \\
= \det(\boldsymbol{I}) - \det[\boldsymbol{F}(j\omega_0)\boldsymbol{T}(j\omega_0)] - e_1 - \cdots e_{n-1} \\
\approx 1 - e_{n-1} \\
= 1 - L_{1,1}(j\omega_0) - L_{2,2}(j\omega_0) - \cdots L_{n,n}(j\omega_0) \\
= 1 - \underbrace{[F_{1,1}(j\omega_0)G_{M,1}(j\omega_0) + F_{1,n+1}(j\omega_0)H_{PSS,1}(j\omega_0)]}_{L_{1,1}(j\omega_0)} \\
- \cdots - \underbrace{[F_{n,n}(j\omega_0)G_{M,n}(j\omega_0) + F_{n,2n}(j\omega_0)H_{PSS,n}(j\omega_0)]}_{L_{n,n}(j\omega_0)}
\end{aligned}
$$

(44)

## REFERENCES

[1] P. Kundur, *Power System Stability and Control*. New York, NY, USA: McGraw-Hill, 1994.

[2] M. A. Laughton, "Matrix analysis of dynamic stability in synchronous multimachine systems," *Proc. IEE*, vol. 113, no. 2, pp. 325–336, Feb. 1966.

[3] J. M. Uudrill, "Dynamic stability calculations for an arbitrary number of interconnected synchronous machines," *IEEE Trans. Power App. Syst.*, vol. PAS-87, no. 3, pp. 835–844, Mar. 1968.

[4] F. P. D. Mello, P. J. Nolan, T. F. Laskowski, and J. M. Undrill, "Coordinated application of stabilizers in multimachine power systems," *IEEE Trans. Power App. Syst.*, vol. PAS-99, no. 3, pp. 892–901, May 1980, doi: 10.1109/TPAS.1980.319717.

[5] V. Arcidiacono, E. Ferrari, and F. Saccomanno, "Studies on damping of electromechanical oscillations in multimachine systems with longitudinal structure," *IEEE Trans. Power App. Syst.*, vol. PAS-95, no. 2, pp. 450–460, Mar. 1976, doi: 10.1109/T-PAS.1976.32124.

[6] J. L. Rodriguez-Amenedo and S. A. Gomez, "Damping low-frequency oscillations in power systems using grid-forming converters," *IEEE Access*, vol. 9, pp. 158984–158997, 2021, doi: 10.1109/ACCESS.2021.3130333.

[7] T. Zhou, Z. Chen, B. Ren, S. Bu, and P. Wang, "Damping torque analysis of VSC-HVDC supplementary damping controller for small-signal stability," *IEEE Access*, vol. 8, pp. 202696–202706, 2020, doi: 10.1109/ACCESS.2020.3036495.

[8] F. P. Demello and C. Concordia, "Concepts of synchronous machine stability as affected by excitation control," *IEEE Trans. Power App. Syst.*, vol. PAS-88, no. 4, pp. 316–329, Apr. 1969, doi: 10.1109/TPAS.1969.292452.

[9] H. A. M. Moussa and Y.-N. Yu, "Dynamic interaction of multimachine power system and excitation control," *IEEE Trans. Power App. Syst.*, vol. PAS-93, no. 4, pp. 1150–1158, Jul. 1974, doi: 10.1109/TPAS.1974.294061.

[10] H. B. Gooi, E. F. Hill, M. A. Mobarak, D. H. Thorne, and T. H. Lee, "Coordinated multi-machine stabilizer settings without eigenvalue drift," *IEEE Trans. Power App. Syst.*, vol. PAS-100, no. 8, pp. 3879–3887, Aug. 1981, doi: 10.1109/TPAS.1981.316983.

[11] P. Pourbeik and M. J. Gibbard, "Damping and synchronizing torques induced on generators by FACTS stabilizers in multimachine power systems," *IEEE Trans. Power Syst.*, vol. 11, no. 4, pp. 1920–1925, Nov. 1996, doi: 10.1109/59.544664.

[12] P. Pourbeik and M. J. Gibbard, "Simultaneous coordination of power system stabilizers and FACTS device stabilizers in a multimachine power system for enhancing dynamic performance," *IEEE Trans. Power Syst.*, vol. 13, no. 2, pp. 473–479, May 1998, doi: 10.1109/59.667371.

[13] M. J. Gibbard, D. J. Vowles, and P. Pourbeik, "Interactions between, and effectiveness of, power system stabilizers and FACTS device stabilizers in multimachine systems," *IEEE Trans. Power Syst.*, vol. 15, no. 2, pp. 748–755, May 2000, doi: 10.1109/59.867169.

[14] P. Pourbeik, M. J. Gibbard, and D. J. Vowles, "Proof of the equivalence of residues and induced torque coefficients for use in the calculation of eigenvalue shifts," *IEEE Power Eng. Rev.*, vol. 22, no. 1, pp. 58–60, Jan. 2002, doi: 10.1109/MPER.2002.4311662.

[15] J. Zhang, C. Y. Chung, and Y. Han, "A novel modal decomposition control and its application to PSS design for damping interarea oscillations in power systems," *IEEE Trans. Power Syst.*, vol. 27, no. 4, pp. 2015–2025, Nov. 2012, doi: 10.1109/TPWRS.2012.2188820.

[16] R. Jalayer and B.-T. Ooi, "Co-ordinated PSS tuning of large power systems by combining transfer function-eigenfunction analysis (TFEA), optimization, and eigenvalue sensitivity," *IEEE Trans. Power Syst.*, vol. 29, no. 6, pp. 2672–2680, Nov. 2014, doi: 10.1109/TPWRS.2014.2314717.

[17] A. R. Messina, J. M. Ramirez, and J. M. C. Canedo, "An investigation on the use of power system stabilizers for damping inter-area oscillations in longitudinal power systems," *IEEE Trans. Power Syst.*, vol. 13, no. 2, pp. 552–559, May 1998, doi: 10.1109/59.667382.

[18] Y. Lin, W. Du, T. Su, and H. Wang, "A simple method of coordinated design of multiple PSSs in multi-machine power systems," in *Proc. APPEEC*, Xi'an, China, Oct. 2016, pp. 1279–1283.

[19] J. C. Mantzaris, A. Metsiou, and C. D. Vournas, "Analysis of inter-area oscillations including governor effects and stabilizer design in," *IEEE Trans. Power Syst.*, vol. 28, no. 4, pp. 4948–4956, Nov. 2013, doi: 10.1109/TPWRS.2013.2251013.

[20] G. Tsourakis, B. M. Nomikos, and C. D. Vournas, "Contribution of doubly fed wind generators to oscillation damping," *IEEE Trans. Energy Convers.*, vol. 24, no. 3, pp. 783–791, Sep. 2009, doi: 10.1109/TEC.2009.2025330.

[21] R. V. de Oliveira, J. A. Zamadei, and C. H. Hossi, "Impact of distributed synchronous and doubly-fed induction generators on small-signal stability of a distribution network," in *Proc. IEEE Power Energy Soc. Gen. Meeting*, Detroit, MI, USA, Jul. 2011, pp. 1–8.

[22] J. Quintero, V. Vittal, G. T. Heydt, and H. Zhang, "The impact of increased penetration of converter control-based generators on power system modes of oscillation," *IEEE Trans. Power Syst.*, vol. 29, no. 5, pp. 2248–2256, Sep. 2014, doi: 10.1109/TPWRS.2014.2303293.

[23] N. Ding, Z. Lu, Y. Qiao, and Y. Min, "Simplified equivalent models of large-scale wind power and their application on small-signal stability," *J. Mod. Power Syst. Clean Energy*, vol. 1, no. 1, pp. 58–64, Jun. 2013, doi: 10.1007/S40565-013-0005-3.

[24] T. Knüppel, J. N. Nielsen, K. H. Jensen, A. Dixon, and J. Østergaard, "Small-signal stability of wind power system with full-load converter interfaced wind turbines," *IET Renew. Power Gener.*, vol. 6, no. 2, pp. 79–91, 2012.

[25] L. P. Kunjumuhammed, B. C. Pal, K. K. Anaparthi, and N. F. Thornhill, "Effect of wind penetration on power system stability," in *Proc. IEEE Power Energy Soc. Gen. Meeting*, Vancouver, BC, Canada, Jul. 2013, pp. 1–5.

[26] D. Gautam, V. Vittal, and T. Harbour, "Impact of increased penetration of DFIG-based wind turbine generators on transient and small signal stability of power systems," *IEEE Trans. Power Syst.*, vol. 24, no. 3, pp. 1426–1434, Aug. 2009, doi: 10.1109/TPWRS.2009.2021234.

[27] W. Du, J. Bi, J. Cao, and H. F. Wang, "A method to examine the impact of grid connection of the DFIGs on power system electromechanical oscillation modes," *IEEE Trans. Power Syst.*, vol. 31, no. 5, pp. 3775–3784, Sep. 2016, doi: 10.1109/TPWRS.2015.2494082.

[28] W. Du, X. Chen, and H. Wang, "Impact of dynamic interactions introduced by the DFIGs on power system electromechanical oscillation modes," *IEEE Trans. Power Syst.*, vol. 32, no. 6, pp. 4954–4967, Nov. 2017, doi: 10.1109/TPWRS.2017.2684463.

[29] Q. Zhang, S. Wu, H. Xu, W. Huang, and D. Gan, "An analysis method for the influence of governors and PSSs on low-frequency oscillation," in *Proc. IEEE 5th Conf. EI2*, Taiyuan, China, Oct. 2021, pp. 4259–4263.

[30] H. F. Wang and W. Du, *Analysis and Damping Control of Power System Low-Frequency Oscillations*. Berlin, Germany: Springer, 2016.

[31] P. W. Sauer and M. A. Pai, *Power System Dynamics and Stability*. Hoboken, NJ, USA: Wiley, 1998.

[32] S. Skogestad and I. Postlethwaite, "Elements of linear system theory," in *Multivariable Feedback Control: Analysis and Design*. London, U.K.: Wiley, 2001, pp. 147–150.

[33] G. F. Franklin, J. D. Powell, and A. Emami-Naeini, "The frequency-response design method," in *Feedback Control of Dynamic Systems*. New York, NY, USA: Pearson, 1994, pp. 353–377.

[34] K. J. Astrom and R. M. Murray, "Frequency domain analysis," in *Feedback Systems: An Introduction for Scientists and Engineers*. Princeton, NJ, USA: Princeton Univ. Press, 2010, pp. 270–283.

[35] Y. Xu, Z. Gu, K. Sun, and X. Xu, "Understanding a type of forced oscillation caused by steam-turbine governors," *IEEE Trans. Energy Convers.*, vol. 35, no. 3, pp. 1719–1722, Sep. 2020, doi: 10.1109/TEC.2020.2995073.

[36] R. Grondin, I. Kamwa, L. Soulieres, J. Potvin, and R. Champagne, "An approach to PSS design for transient stability improvement through supplementary damping of the common low-frequency," *IEEE Trans. Power Syst.*, vol. 8, no. 3, pp. 954–963, Aug. 1993.

[37] J. Zhou, T. Zheng, and D. Gan, "Value-set-based power system robust stability analysis: Further results," *IEEE Trans. Power Syst.*, vol. 34, no. 2, pp. 1383–1392, Mar. 2019, doi: 10.1109/TPWRS.2018.2878444.

[38] R. A. Horn and C. R. Johnson, "Review and miscellanea," in *Matrix Analysis*. Cambridge, U.K.: Cambridge Univ. Press, 1990, pp. 13–15.

[39] I. C. F. Ipsen and R. Rehman, "Perturbation bounds for determinants and characteristic polynomials," *SIAM J. Matrix Anal. Appl.*, vol. 30, no. 2, pp. 762–776, Jan. 2008, doi: 10.1137/070704770.

**ZHEMING ZHANG** received the M.S. degree from the School of Electrical Engineering, Xi'an Jiaotong University, China, in 2018. He is currently with Yunnan Power Grid Corporation, where he performs power system operations studies.



**QINGBO ZHANG** received the M.S. degree in electrical engineering from the Stevens Institute of Technology, Hoboken, NJ, USA, in 2017. She is currently pursuing the Ph.D. degree in electrical engineering with Zhejiang University, Hangzhou, China. Her main research interest includes power system stability analysis and control.



**DEQIANG GAN** (Senior Member, IEEE) received the Ph.D. degree in electrical engineering from Xi'an Jiaotong University, China, in 1994. He held research positions with Ibaraki University, the University of Central Florida, and Cornell University, from 1994 to 1998. He was with ISO New England Inc., from 1998 to 2002. Since 2002, he has been with the Faculty of Zhejiang University. He visited The University of Hong Kong, in 2004, 2005, and 2006. His research interest includes power system stability and control. He served as the Editor for *European Transactions on Electrical Power* (2007–2014).



**JINQIU LI** received the integrated M.S. degree from Chongqing University and California State University, Sacramento, CA, USA, in 2018. Since 2018, he has been with Yunnan Power Grid Corporation. His research interest includes power system stability and control.



**YAO LUO** received the M.S. degree from the School of Electrical Engineering, Xi'an Jiaotong University, in 2019. Since 2019, she has been with Yunnan Power Grid Corporation. Her research interest includes power system stability analysis.

●　●　●